HHS Public Access

Author manuscript

Sci Transl Med. Author manuscript; available in PMC 2017 September 27.

Published in final edited form as:

Sci Transl Med. 2016 September 14; 8(356): 356ra120. doi:10.1126/scitranslmed.aaf4363.

Treatment of otitis media by transtympanic delivery of antibiotics

Rong Yang[1], **Vishakha Sabharwal**[2], **Obiajulu S. Okonkwo**[1], **Nadya Shlykova**[2], **Rong Tong**[1,*], **Lily Yun Lin**[1], **Weiping Wang**[1], **Shutao Guo**[1], **John J. Rosowski**[3], **Stephen I. Pelton**[2], and **Daniel S. Kohane**[1,†]

[1]Laboratory for Biomaterials and Drug Delivery, Department of Anesthesiology, Division of Critical Care Medicine, Boston Childrens Hospital, Harvard Medical School, Boston, MA 02115, USA

[2]Division of Pediatric Infectious Diseases, Maxwell Finland Laboratory for Infectious Diseases, Boston Medical Center, Boston, MA 02118, USA

[3]Department of Otology and Laryngology, Eaton-Peabody Laboratories, Massachusetts Eye and Ear Infirmary, Boston, MA 02114, USA

Abstract

Otitis media is the most common reason U.S. children receive antibiotics. The requisite 7- to 10-day course of oral antibiotics can be challenging to deliver in children, entails potential systemic toxicity, and encourages selection of antimicrobial-resistant bacteria. We developed a drug delivery system that, when applied once to the tympanic membrane through the external auditory canal, delivers an entire course of antimicrobial therapy to the middle ear. A penta-block copolymer poloxamer 407–polybutylphosphoester (P407-PBP) was designed to flow easily during application and then to form a mechanically strong hydrogel on the tympanic membrane. U.S. Food and Drug Administration–approved chemical permeation enhancers within the hydrogel assisted flux of the antibiotic ciprofloxacin across the membrane. This drug delivery system completely eradicated otitis media from nontypable *Haemophilus influenzae* (*NTHi*) in 10 of 10 chinchillas, whereas only 62.5% of animals receiving 1% ciprofloxacin alone had cleared the infection by day 7. The hydrogel system was biocompatible in the ear, and ciprofloxacin was undetectable systemically (in blood), confirming local drug delivery and activity. This fast-gelling hydrogel could improve compliance, minimize side effects, and prevent systemic distribution of antibiotics in one of the most common pediatric illnesses, possibly minimizing the development of antibiotic resistance.

†Corresponding author: daniel.kohane@childrens.harvard.edu.

*Present address: Department of Chemical Engineering, Virginia Polytechnic Institute and State University, Blacksburg, VA 24061, USA.

Author contributions: R.Y. and R.T. synthesized the polymer. R.Y. conducted FTIR. R.Y. and O.S.O. conducted in vitro and ex vivo experiments. R.Y., O.S.O., and W.W. performed cell culture. R.Y. and W.W. conducted TEM. S.G. conducted NMR. R.Y., V.S., O.S.O., and N.S. performed in vivo experiments. R.Y., O.S.O., and J.J.R. performed ABR tests. R.Y., V.S., O.S.O., R.T., L.Y.L., J.J.R., S.I.P., and D.S.K. contributed to study design. R.Y., V.S., S.I.P., J.J.R., and D.S.K. performed data analysis and interpretation. R.Y., D.S.K., and S.I.P. drafted the article and/or edited it critically for important intellectual content.

Competing interests: The authors declare that they have no competing interests. A provisional patent has been filed (C1233.70091US00) pertaining to the results presented in the paper.

Data and materials availability: All data for this study have been included in this article. All materials are commercially available.

INTRODUCTION

With 12 million to 16 million physician visits per year in the United States attributed to otitis media (OM), OM is the most frequently diagnosed illness in children (1). Acute OM is highly prevalent in infants and young children; more than 90% have an episode before age 5 (2, 3), and it is the most common reason for prescribing antimicrobial agents to U.S. children. In the developing world, chronic suppurative OM frequently results in permanent hearing sequelae and is estimated to result in more than 25,000 deaths worldwide because of intracranial complications (4). Current therapy for acute OM typically consists of a 10-day course of broad-spectrum oral antibiotics. Frequent recurrences of this disease (40% of children have four or more episodes of acute OM and 26% require tympanostomy tube insertion by age 7) (5, 6) are believed to be partially responsible for the ongoing increase in antibiotic resistance among pathogenic bacteria. Furthermore, the systemic administration of antibiotics often results in side effects, including diarrhea, dermatitis, vomiting, and oral thrush (1). Administration of oral antibiotics in young children can be very challenging for caregivers. Incomplete compliance with the current multidose, multiday regimens can compromise efficacy and increase the potential for bacterial resistance.

Local, sustained delivery of active therapeutics directly to the middle ear for the treatment of OM could potentially minimize systemic exposure and its side effects and allow for substantially higher middle ear drug concentrations than from systemic administration. However, the tympanic membrane (TM), although only about 100 μm thick, presents a barrier that is largely impermeable to all but the smallest lipophilic molecules because of its keratin- and lipid-rich stratum corneum (7). One approach to overcome this permeation barrier is by using chemical permeation enhancers (CPEs), which are U.S. Food and Drug Administration (FDA)–approved for transdermal drug delivery (8). We have previously demonstrated that CPEs can increase drug flux across the chinchilla TM ex vivo (9). However, the success of using CPEs to enable antibiotic flux across the TM depends on developing a delivery vehicle, which we pursued in this study. Such a hydro-gel delivery system would need to conform to the TM to maximize drug flux, to have rapid gelation kinetics (especially relevant for delivering to children), to provide controlled release of the antibiotic over 7+ days, to leave minimal residue in the outer ear canal, and to be biocompatible in the ear. Such a system could enable single-dose application by the pediatrician at the time of diagnosis and thus avoid the challenges encountered by parents during conventional multidose oral antibiotic therapy.

Hydrogels are suitable candidates for such a system. Several polymer types can provide excellent fluidity during application followed by in situ gelation [reviewed in (10)]. Reverse thermal gelation is one mechanism for in situ gelation, whereby a liquid forms a gel when encountering a higher temperature [reviewed in (10, 11)]. Although hydrogels may not be ideal for providing extended drug release, we hypothesize that the relatively negligible fluid turnover in the outer ear will limit drug diffusion away from the depot except through the CPE-permeabilized TM. Additionally, hydrogels often have excellent biocompatibility in humans (10, 12, 13).

Here, we demonstrate the development of a hydrogel containing an antibiotic and CPEs, which enhance antibiotic flux across the TM. The hydrogel effectively eradicated acute OM due to *Haemophilus influenzae* (*NTHi*) in a chinchilla model. We chose ciprofloxacin as the antibiotic because it is a small molecule, is moderately hydrophobic, can be dissolved at relatively high concentration in aqueous solution at acidic pH (14), and has a broad antibacterial spectrum. Ciprofloxacin is also currently used clinically to treat acute otorrhea in children with tympanostomy tubes. This drug delivery platform allows antibiotics to transport directly into the middle ear to treat OM, one of the most common pediatric illnesses. A single dose delivered by a pediatrician, at the time of diagnosis, would contain an entire antibiotic course. This treatment would improve patient compliance, avoid systemic antibiotic exposure, and thus reduce side effects and the development of antimicrobial resistance.

RESULTS

CPEs reduced the mechanical strength of poloxamer 407

We designed the hydrogel drug delivery systems to contain the antibiotic ciprofloxacin (Cip), CPEs, and the copolymer poloxamer 407–polybutylphosphoester (P407-PBP). The formulations are referred to as Cip-CPE-*z*% [P407-PBP], where $z = 1$, 12, or 18% (w/v) of the polymer. Unless specified otherwise, the concentrations of CPEs were as follows: 2% (w/v) limonene (LIM), 1% (w/v) sodium dodecyl sulfate (SDS), and 0.5% (w/v) bupivacaine (BUP). 3CPE denotes a combination of all three. The concentration of ciprofloxacin was always 1% (w/v). The concentrations of CPEs and ciprofloxacin were adopted from our previous report (9). If a component was absent from a formulation, it was omitted from the above nomenclature.

A key aspect of the design was that the hydrogel containing antibiotics and CPEs should flow readily into place, such as through an otoscope, and then promptly become a gel that maintains physical integrity throughout the course of treatment. Previously, we had used an 18% aqueous solution of commercially available P407 (18%[P407]), which demonstrated reverse thermal gelation, as the vehicle to deliver the antibiotic ciprofloxacin with CPEs to the TM (9). For 18%[P407], the storage (G') and loss (G'') moduli (measured by linear oscillatory shear rheology at 100 $rads^{-1}$, 1% strain, and 1°C/min) were ~1 kPa at room temperature; it behaved as a viscous liquid. G' and G'' demonstrated sharp increases at temperatures above 27°C and plateaued at ~6 and 4 kPa, respectively (Fig. 1A), demonstrating solid-like behavior. However, when 3CPE was added to the P407 solution at concentrations which we previously used to enhance permeation across the TM (9), G' and G'' of the formulation were less than 2 kPa over the temperature range of 20° to 40°C (Fig. 1A); that is, the material did not form a gel in the presence of 3CPE.

The suppression of gelation could be attributed to the inhibitory effects of CPEs on the micellization of P407 molecules. Above the critical micellization temperature, P407 molecules assemble into micelles with a core containing the hydrophobic polypropylene oxide blocks and a shell of the hydrated polyethylene oxide blocks. As the temperature increases, the micelles form a liquid-crystalline gel with body-centered cubic structure (15). The formation of 100- to 150-nm-diameter micelles at room temperature in a 1% P407

solution without CPEs (1%[P407]) was documented by transmission electron microscopy (TEM) (Fig. 1B). No micelles formed when CPEs were added to the P407 (3CPE-1% [P407]). Suppression of micelle formation has been attributed to small molecules (in this case, CPEs) binding cooperatively on block copolymer molecules, rendering the hydrophobic block hydrophilic (16). The shear rheology results and TEM images were consistent with our pilot observation by otoscopy in two of two chinchillas that Cip-3CPE-18%[P407] did not maintain structural integrity on the TM.

Pentablock copolymer P407-PBP was designed to maintain mechanical strength

The deleterious effects of the CPEs on the mechanical properties of P407 were addressed by adding hydrophobic end blocks, which facilitated gelation at elevated temperatures via hydrophobic interactions (Fig. 1, C and D) (17, 18). Specifically, we decorated the ends of P407 with an aliphatic polyphosphoester (PPE), one of a class of generally biocompatible and biodegradable polymers (17, 19). Block copolymers of PPE with aliphatic side chains demonstrate reverse thermal gelation (17, 20), likely owing to the breaking of hydrogen bonding with ambient water molecules at elevated temperature (20). Their side chains (such as methyl, ethyl, and isopropyl) can be changed easily to tune the hydrophobicity and temperature responsiveness (21). We chose butyl side chains to enhance hydrophobicity and thus increase the thermodynamic driving force for gelation (22).

The pentablock copolymer P407-PBP with *n*- or *s*-butyl side groups (Fig. 1, C to E) was synthesized via ring-opening polymerization in the presence of an organocatalyst, 1,8-diazabicyclo[5.4.0]undec-7-ene (DBU) (Fig. 1C). Fourier transform infrared spectroscopy (FTIR) confirmed the presence of PBP moieties (Fig. 1E) (23), which were present in the spectrum of the ring-opening polymerization product but not the reactant P407, indicating the successful addition of PPE blocks. Increased molecular weight, demonstrated by gel permeation chromatography (GPC) (table S1), indicated that P407 was chemically modified by either *n*- or *s*-butyl PBP blocks and not simply mixed with those PBP blocks. The number-average molecular weight (M_n) measured by nuclear magnetic resonance (NMR) agreed with that calculated from the chemical formulae (table S1) and was confirmed with GPC. In our synthetic scheme, a small degree of polymerization (DP) was targeted to avoid gelation at or below room temperature and to facilitate degradation of the hydrogel. The actual DP of the PPE blocks was determined to be 5 (fig. S1). A smaller DP of 2.5 resulted in a high gelation temperature and poor shear strength (Fig. 1F). P407-PBP with an *n*-butyl group and a DP of 5 was used in subsequent studies because it gelled at lower temperature and it has greater shear moduli than those made with *s*-butyl groups (Fig. 1F).

CPEs enhanced the mechanical strength of P407-PBP

P407-PBP had faster gelation kinetics than unmodified P407. The solution to gel (sol-gel) transition occurred ~7 s after Cip-3CPE-18%[P407-PBP] was submerged in a water bath at 37°C, whereas Cip-3CPE-18%[P407] remained as a solution for 48 s (movie S1). Cip-18% [P407] and Cip-18% [P407-PBP] (in the absence of 3CPE) demonstrated identical gelation kinetics (movie S2). Gelation of P407-PBP was not hindered by the inclusion of 3CPE. G′ and G″ of Cip-18%[P407-PBP] were ~0.3 and 1.0 kPa, respectively, at room temperature (Fig. 1A). G′ and G″ both increased gradually in the temperature range 27° to 38°C and

became 7.8 and 5.0 kPa, respectively, near body temperature. The sol-gel transition temperature was ~33°C. Introduction of 3CPE to Cip-18%[P407-PBP] increased its G′ by more than 2.5-fold (Fig. 1A). G′ and G″ increased from close to zero at room temperature to 20 and 1.3 kPa, respectively, at 37°C. The polymer solution exhibited a sol-gel transition temperature of 20°C. Micelles were observed at low polymer concentrations (1%) for P407-PBP even in the presence of CPEs (Fig. 1B).

To evaluate the effect of individual CPEs on temperature-dependent mechanical properties, we added 1% SDS, 2% LIM, or 0.5% BUP separately to Cip-18%[P407-PBP] (Fig. 2A; data for each CPE are in fig. S2). LIM reduced the gelation temperature of Cip-18%[P407-PBP] by 14°C, increased G′ by 10.5 kPa, and decreased G″ by 4.1 kPa, such that they were very similar to those for Cip-3CPE-18%[P407-PBP] (Fig. 1A and fig. S2). SDS lowered the gelation temperature of Cip-18%[P407-PBP] by ~1.5°C but did not affect the plateau values of G′ and G″. BUP had minimal effects on the mechanical properties and gelation temperature of Cip-18%[P407-PBP]. These data indicated that the influences of CPEs were dominated by the effects of LIM.

Extruding the formulations of Cip-3CPE-18%[P407-PBP] (movie S3) and Cip-3CPE-15%[P407-PBP] (movie S4) through a catheter to mimic application in vivo was challenging, presumably because the friction generated during injection was enough to heat the formulations and clog the catheter. For example, Cip-3CPE-15%[P407-PBP] was hard to push through a 20-gauge catheter and extruded as a gel rather than a viscous liquid, which made in vivo placement on the chinchilla TM difficult. Therefore, for in vivo work, we selected Cip-3CPE-12%[P407-PBP] because its sol-gel transition was clear (G′ > G″ at body temperature) (Fig. 2, B and C, and fig. S2E) and it did not gel after extrusion through a 20-gauge, 1.8-inch catheter at room temperature (movie S5).

Transtympanic permeation was enhanced despite slowed release from the hydrogel

The design of our formulation entailed two components: CPEs, which were expected to increase drug flux across the TM (9), and the hydrogel, which was expected to slow flux yet prolong treatment for the duration that is needed to clear infection. The effects of the hydrogel and 3CPE on the transport rate of ciprofloxacin were studied by quantifying (i) in vitro diffusion from the bulk hydrogel matrix (albeit in infinite sink conditions, which are unlikely to exist on the TM surface) and (ii) ex vivo permeation across the TM. In vitro release experiments showed that P407-PBP slowed drug release compared to the free drug solution (Fig. 3A). Incorporation of 3CPE caused further slowing of drug release. However, the magnitude of ciprofloxacin released from Cip-3CPE-12%[P407-PBP] was >30% greater than that from Cip-3CPE-12%[P407].

Drug transport across the TM was studied ex vivo in auditory bullae excised from healthy chinchillas. Inclusion of 3CPE enhanced the flux across the TM from a 1% ciprofloxacin solution more than 4-fold and from Cip-12%[P407-PBP] more than 10-fold (Fig. 3B). Conversely, the presence of a hydrogel tended to decrease flux across the TM—an effect that could be overcome by the incorporation of CPEs. The ex vivo model could not be used to demonstrate the presumed principal utility of the hydrogel, which was to prolong the

duration of drug flux across the TM by creating a stable depot system because the TMs degraded after ~48 hours at 37°C.

Hydrogel drug delivery system cured OM in vivo in chinchillas

OM due to *NTHi* was established in chinchillas after direct inoculation of the virus into the middle ear. The ears were then treated with 200 μl of test material deposited through the external canal on to the TM. OM was defined as nonzero colony-forming units (CFU) in middle ear fluid aspirated through the dorsal aspect of the auditory bullae, not through the TM. In animals treated with 1% ciprofloxacin alone, infection was detectable in 25% animals on days 1 and 3, but by day 7, only 62.5% animals had cleared the infection (Fig. 4A), an unacceptably low cure rate (24). The OM clearance rate was similarly low, plateauing at 60% of animals treated with Cip-3CPE-18%[P407] (Fig. 4A). In contrast, OM was cleared in 10 of 10 animals treated with Cip-3CPE-12%[P407-PBP] within 24 hours after the application of the formulation (Fig. 4A). The time course of the average number of colonies (CFU/ml) in middle ear fluid from animals in both groups is provided in Fig. 4B.

The 100% OM cure rate in animals treated with Cip-3CPE-12%[P407-PBP] may be explained by the time course of ciprofloxacin levels in the middle ear (Fig. 4C). The minimum inhibitory concentration (MIC) of ciprofloxacin for treating *NTHi* is 0.1 to 0.5 μg/ml (25, 26). The concentration of ciprofloxacin peaked at day 1 (39.1 μg/ml in animals treated with Cip-3CPE-12%[P407-PBP] and 4.2 μg/ml in those treated with 1% ciprofloxacin solution). Three days after administration of the formulations, ciprofloxacin was still above the MIC (3.06 μg/ml) in the middle ears of animals that received Cip-3CPE-12%[P407-PBP], whereas the ciprofloxacin concentration dropped to zero in animals treated with 1% ciprofloxacin solution. Seven days after administration, the ciprofloxacin concentration was still 1.2 μg/ml in the middle ear fluid of animals treated with Cip-3CPE-12%[P407-PBP]. No recurrence of OM was observed within 7 days; in children with acute OM, this is a strong indication of cure (27).

The effect of Cip-3CPE-12%[P407-PBP] on hearing sensitivity was assessed by auditory brainstem responses (ABRs). Placement of 200 μl of the gel on the TM caused a 16- to 24-dB positive shift of the ABR threshold (worsening of hearing) to clicks and tone bursts of frequencies from 0.5 to 16 kHz, with an average of 18 ± 8 dB across all frequencies (Fig. 4D). This mild hearing loss is comparable to the effect of cerumen (commonly known as “earwax”) on hearing in humans (28), and because it is likely mechanically induced, hearing is expected to return to normal after the gel degrades. The TM does return to normal histologically (Fig. 5).

The hydrogel drug delivery system was biocompatible in the ear, with no systemic drug distribution in chinchillas

Tissue toxicity is an important consideration because CPEs have been shown to disrupt the stratum corneum, which is part of the TM (29). The specific combination of 3CPE was chosen because it enhances permeation across the TM and is nontoxic in vivo in chinchillas and human (9, 30). Cytotoxicity of the polymer and 3CPE was evaluated in three cell lines that are representative of cell types in the auditory system: human dermal fibroblasts (hFBs),

PC12 cells (a pheochromocytoma cell line frequently used to test neurotoxicity), and normal adult human primary epidermal keratinocytes from abdominal skin. P407-PBP itself showed little toxicity after 1 day, but only 20% of keratinocytes survived until day 3 (Fig. 6). The presence of 3CPE and ciprofloxacin increased the cytotoxicity for all cell types and time points.

Nevertheless, the gels were biocompatible in the ear in vivo. TMs excised 7 days after treatment with 200 μl of Cip-3CPE-12%[P407-PBP] were histologically similar to healthy TMs that had not been exposed to any treatment (Fig. 5A): 10 to 20 μm thick and without tissue injury, necrosis, or inflammatory cells. Untreated TMs extracted after 7 days of infection were about 10 times thicker than normal (Fig. 5A) and exhibited an acute inflammatory response with diffuse edema and dense infiltration by inflammatory cells (Fig. 5A, lower left panel). The single-dose treatment with Cip-3CPE-12%[P407-PBP] could reverse the prominent inflammatory response caused by *NTHi* (Fig. 5B); TMs treated with the gel formulation appeared indistinguishable from normal (Fig. 5A). No tissue injury, necrosis, or inflammatory cells were observed. Bacteria (next to the umbo) were eradicated after 1 week of treatment with Cip-3CPE-12%[P407-PBP](Fig. 5B).

Gels were adherent to the TMs 7 days after application but had degraded completely within 3 weeks. Ciprofloxacin was undetectable in plasma samples from blood obtained in the transverse sinus (table S2). Given the proximity of that location to the auditory bullae, the absence of ciprofloxacin suggested that no detectable systemic exposure of antibiotics occurred.

The hydrogel drug delivery system could work with thicker human TM

To assess the potential effect of the thicker human TM on diffusion of ciprofloxacin, we used an established transient diffusion model for the stratum corneum (31), which provided the principal resistance to transport (7, 31). We assumed that (i) the diffusion coefficients of ciprofloxacin were identical in chinchilla and human stratum corneum, (ii) the thickness of the human TM is thicker than the chinchilla TM (that is, ~47 μm versus 4.7 μm), and (iii) the ratio of the diffusion coefficients for infected and healthy TM is independent of the formulation used. The apparent diffusion coefficients across human TM with OM for ciprofloxacin from 1% ciprofloxacin solution and Cip-3CPE-18%[P407-PBP] were determined to be 4.60×10^{-16} m^2 s^{-1} and 2.11×10^{-15} m^2 s^{-1}, respectively (table S3), by fitting the drug transport profiles (Fig. 3B and fig. S3) to a steady-state model (31).

With these diffusion coefficients, the transient model predicted that ~417 μg of ciprofloxacin would permeate across a human TM with OM during a 7-day treatment with Cip-3CPE-18% [P407-PBP]. Assuming that there was no uptake of ciprofloxacin by bacteria or the patient and that the volume of the infant middle ear is 0.45 ml (32), the MIC of *NTHi* [0.1 to 0.5 μg/ml (25, 26)] could be achieved within the first day (fig. S3). In contrast, the 1% ciprofloxacin solution would require 40 hours of contact with the TM to reach the lower bound of MIC of *NTHi* in the middle ear.

DISCUSSION

We have developed an ototopical acute OM treatment platform that, although applied only once, provided local sustained delivery of antibiotics directly to the middle ear for at least 7 days, eradicating infection and restoring the TM to normal. The transport of antibiotics directly to the middle ear remained local, without detectable systemic distribution, and could thus avoid side effects and antibiotic resistance. The gel had a modest negative effect on hearing, presumably due to its presence on the TM. This would likely resolve as the gel disappeared completely within 3 weeks of administration. The optimized injectable gel containing ciprofloxacin, 3CPE, and 12% polymer was biocompatible in vivo. The formulation would allow a pediatrician, at the time of diagnosis, to deliver a single dose of antibiotics to the TM that provides an entire course of treatment, which could improve compliance.

The central point of this work was the demonstration of a formulation that can treat OM transtympanically. CPEs enhanced transtympanic flux, which was important given that the hydrogel itself reduced drug flux across the TM. The fact that Cip-3CPE containing 12% [P407-PBP] was more successful than 18%[P407] in eradicating OM suggests the importance of the ability of the formulation to persist at the TM; Cip-3CPE-12%[P407-PBP] was present for at least 1 week, whereas Cip-3CPE-18%[P407] was gone after 1 day. Exactly which CPE or CPE combination is optimal, and at what concentration, remains to be determined.

It was somewhat surprising that ciprofloxacin solution alone had any therapeutic effect on OM, given that the TM is relatively impermeable to small molecules (7, 9, 33) and ototopical antibiotics are only used for middle ear disease in situations where the TM has been breached (for example, with myringotomy tubes) (34). The effect of ciprofloxacin drops in OM may be explained by the fact that the TM became 5- to 31-fold more permeable to drug flux in OM despite also becoming five times thicker than in healthy animals. Even so, the cure rate from ciprofloxacin solution was unsatisfactory [one would prefer >88% based on FDA 2001 Advisory Committee recommendation (35)] and would likely be even lower with the thicker TMs in humans (36). Human TMs are on average about 10-fold thicker than chinchilla TMs, with great variability (36, 37). Our modeling data indicated that a ciprofloxacin solution is unlikely to be effective in human OM. Moreover, it is unlikely that a drop of free liquid would stay at the TM for that duration in a toddler.

As occurs with transdermal drug delivery systems, the CPEs most likely disrupt the stratum corneum of the TM, thus increasing its permeability to ciprofloxacin (29, 38) but also potentially causing tissue injury. Biocompatibility in vivo was excellent, even though there was considerable cytotoxicity in vitro. This in vitro–in vivo discrepancy is not uncommon (39). Degradation of the gel at the TM was likely mediated through hydrolytic cleavage of the phosphoester bonds in the backbone and the side chains, which can occur spontaneously under physiological conditions, or catalytically by enzymatic digestion of phosphate linkages (40).

In infected chinchillas treated with Cip-3CPE-12%[P407-PBP], the concentration of ciprofloxacin in the middle ear peaked after 1 day and was maintained above the MIC of *NTHi* throughout the 7-day treatment. The peak concentration was almost six times as high as from 1% ciprofloxacin solution. The high and sustained concentrations from Cip-3CPE-12%[P407-PBP] suggest that this formulation could be effective in treating otopathogens with higher MICs, and that this treatment could work across the range of middle ear volumes seen from infancy to adulthood, although changes in volume administered or drug concentration might be needed. Although there was a high local concentration, the absence of detectable drug in the bloodstream is potentially important for the avoidance of systemic toxicity and for mitigating the public health hazard of causing emergence of drug-resistant bacteria. Avoiding systemic exposure is particularly important with ciprofloxacin because it is not currently used systemically in general pediatric practice because of its potential harm to pediatric musculoskeletal systems (41). The widespread use of systemic antibiotics against a disease of such high prevalence and recurrence as OM is believed to be partially responsible for the ongoing increase in antibiotic resistance among pathogenic bacteria in the nasopharynx (42). The effective sustained local therapy developed here could address the issue of compliance and affect the development of resistance and chronic suppurative OM. If this therapy could impact biofilm formation, it could potentially reduce the need for tympanostomy tube placement (devices implanted in the TM to enhance middle ear drainage in recurrent OM).

Despite the recognized correlation between results obtained with the chinchilla animal model and those from human trials (43), it is possible that there might be discrepant results in humans. Also, the fact that there was no detectable systemic distribution of antibiotics does not exclude the possibility of antibiotic drainage into the nasopharynx, which could lead to the development of antibiotic-resistant bacteria. Our formulation could eradicate *NTHi*, which has been identified in more than 60% of children with OM (44), but there are other potential otopathogens. The gel caused a minor deficit in hearing immediately (minutes) after application. Given the timing, the deficit can only be due to a mechanical conductive problem, which would be expected to resolve once the gel is gone. That hearing returns to normal will need to be demonstrated definitively.

We have developed a noninvasive, single-dose, local antibiotic treatment regimen and demonstrated its efficacy in the standard chinchilla animal model. The CPEs used are FDA-approved excipients. Ciprofloxacin was used here because of its broad spectrum of activity against relevant bacteria and because of its effectiveness in OM in children with myringotomy tubes (45). The thermosensitive polymer used here is a chemical derivative of FDA-approved poloxamers. Nonetheless, its safety—and that of the formulation as a whole—may have to be demonstrated in healthy human volunteers, as a preliminary to trials in patients with OM. This delivery system is likely compatible with a range of different antibiotics, should a drug other than ciprofloxacin be necessary.

MATERIALS AND METHODS

Study design

Our objective was to develop a noninvasive, transtympanic drug delivery platform for OM. We focused on developing and evaluating formulations containing CPEs and an antibiotic. The experiments compared the effect of the polymer matrix and incorporation of CPEs on TM permeability and OM cure rate. For the ex vivo experiments, a sample size of four for each formulation was chosen, which would provide 80% power to detect 50% differences in flux based on power analysis using the nonparametric Friedman test (version 7.0, nQuery Advisor, Statistical Solutions). Sample sizes of 8 to 10 were used for the in vivo experiments, which were supported by our published experience (46). During ex vivo experiments, data collection was stopped after 48 hours due to microbial growth on harvested TM, whereas, during in vivo experiments, data collection was stopped after 7 days because OM would either be cleared or cause the animal severe illness that required euthanasia. In vivo experiments were blinded. The information regarding whether the animal was infected or healthy and regarding which formulation was administered were kept by two separate research groups and not shared until all data analysis was done. Animals were assigned treatment groups at random.

Animal maintenance

Healthy adult male chinchillas weighing 500 to 650 g were purchased from Ryerson Chinchilla Ranch and cared for in accordance with protocols approved institutionally and nationally. Experiments were carried out in accordance with the Boston Children's Hospital, Boston University Medical Center, and Massachusetts Eye and Ear Infirmary Animal Use Guidelines and approved by each institution's Institutional Animal Care and Use Committee (IACUC).

Synthesis of butoxy-2-oxo-1,3,2-dioxaphospholane

2-Chloro-2-oxo-1,3,2-dioxaphospholane (COP), *n*-butanol, 2-ethyl-1-butanol, and anhydrous tetrahydrofuran (THF) were used as received from Sigma-Aldrich. Butoxy-2-oxo-1,3,2-dioxaphospholane (BP) was prepared by condensation reaction of COP and *n*-butanol or 2-ethyl-1-butanol. COP (5.0 g, 35 mmol) in anhydrous THF (50 ml) was added to a stirring solution of *n*-butanol or 2-ethyl-1-butanol (2.6 g, 35 mmol) and trimethylamine (TEA, 3.9 g, 39 mmol) in anhydrous THF (100 ml) at 0°C dropwise. The reaction mixture was stirred in an ice bath for 12 hours upon completed addition. Upon complete conversion of COP, the reaction mixture was filtered and the filtrate was concentrated. The concentrated filtrate was purified by vacuum distillation under reduced vacuum to yield a viscous colorless liquid.

Synthesis of P407-PBP

Kolliphor P407 microprilled was from BASF. P407-PBP was synthesized by ring-opening polymerization of BP with P407 as the macro-initiator in the presence of an oranocatalyst (DBU; Sigma-Aldrich) at −20°C (47). P407 (8.1 g, 0.56 mmol) and BP (1.0 g, 5.6 mmol) in anhydrous dichloromethane (DCM; 0.5 ml) were added to a flame-dried Schlenk flask (10

ml) equipped with a stir bar. The reaction mixture was flushed with nitrogen gas for 5 min while immersed in an ice bath with saturated NaCl solution. A solution of DBU in anhydrous DCM (0.13 g, 0.84 mmol) was added to the stirring solution via a syringe dropwise while maintaining the reaction under nitrogen gas atmosphere. Upon completion of the reaction, excess amount of acetic acid in DCM was added to the reaction mixture to quench the reaction. The product was purified by precipitation into ether (three times) and dried under vacuum to obtain a white powder product. Molecular weight (M_n) of the product was measured with NMR and GPC. M_n measured by GPC was ~30% higher than that measured using NMR [a discrepancy well documented (48) and attributed to the different chain configurations of the P407-PBP from standard (polystyrene)].

Hydrogel formation

P407-PBP hydrogel formulations were made by adding powdered polymers to aqueous solutions. Gels of varying P407-PBP weight percentage (10 to 18%) can be prepared by simple dissolution in a cold room to allow better solubility. Hydrogel formulation in scintillation vials was immersed in a water bath kept at 37°C with continuous stirring (200 rpm). The time it took the stir bar to stop rotating after immersion was recorded as the gelation time. Gelation temperature was quantified using linear oscillatory shear rheology measurements (100 $rads^{-1}$, 1% strain, and 1°C/min). Gelation temperature was taken as the temperature at which G′ becomes greater than G″. The changes of G′ and G″ over temperatures ranging from 0°C to above body temperature were recorded to reflect changes in mechanical properties.

In vitro release studies

The release of ciprofloxacin from each formulation was measured using a diffusion system. Transwell membrane inserts (0.4-μm pore size and 1.1-cm^2 area; Costar) and 24-well culture plates were used as the donor and acceptor chambers, respectively. Two hundred microliters of each formulation was pipetted directly onto prewarmed filter inserts to obtain a solid hydrogel. Filter inserts (donor compartments) with formed gels were suspended in wells (acceptor compartments) filled with prewarmed phosphate-buffered saline (PBS), and the plates were then incubated in an oven (37°C). At each time point (0.5, 1, 2, 6, 12, 24, and 48 hours), 1-ml aliquots of the PBS-receiving media were sampled and inserts were sequentially moved into a new well with fresh PBS. Aliquots were suspended in acetonitrile/PBS (70:30) to ensure total drug dissolution. Sample aliquots were chromatographically analyzed with high-performance liquid chromatography (HPLC) to determine ciprofloxacin concentrations (λ = 275 nm). More details regarding the ciprofloxacin measurement and HPLC conditions can be found in (9). Experiments were performed in quadruplicate.

Ex vivo TM permeation

The cross-TM permeation rate of ciprofloxacin was determined with auditory bullae harvested from healthy chinchillas. All formulations were applied into the bullae kept at 37°C and deposited onto the TMs. The volume applied was 200 μl, which translates to 2 mg of ciprofloxacin. Permeation of ciprofloxacin across TM into the receiving chamber was quantified using HPLC. Detailed information regarding TM harvesting, TM electrical

resistance measurement, and configuration of the ex vivo permeation experiment can be found in (9).

Cytotoxicity analysis

Cell viabilities were evaluated with an assay of a mitochondrial metabolic activity, CellTiter 96 AQ_{ueous} One Solution Cell Proliferation Assay (Promega Corp.), that uses a tetrazolium compound [3-(4,5-dimethyl-2-yl)-5-(3-carboxymethoxyphenyl)-2-(4-sulfophenyl)-2*H*-tetrazolium, inner salt (MTS)] and an electron coupling reagent (phenazine ethosulfate). On days 1 and 3 of the culture, hFB, PC12, and normal adult human primary epidermal keratinocytes (American Type Culture Collection) were incubated with CellTiter 96 AQ_{ueous} One Solution for 120 min at 37°C. The absorbance of the culture medium at 490 nm was immediately recorded with a 96-well plate reader. The quantity of formazan product (converted from tetrazole) as measured by the absorbance at 490 nm is directly proportional to cell metabolic activity in culture. Planar cultures on 24-well plate were used as controls. Cell viability was confirmed using a LIVE/DEAD Viability/Cytotoxicity Kit (Molecular Probes, Invitrogen). Cells were incubated with calcein-AM (acetoxymethyl) (1 μM) and ethidium homodimer-1 (2 μM) for 30 min at 37°C to label live and dead cells, respectively. Cell viability was calculated as live cells/(live cells + dead cells) × 100.

ABR measurements

ABR experiments were conducted with a custom-designed stimulus generation and measurement system built around the National Instruments software (LabVIEW) and hardware, as described in Supplementary Materials and Methods.

NTHi OM chinchilla model

All procedures and manipulations were performed using sedation analgesia with a mixture of ketamine and xylazine given intramuscularly in accordance with approved IACUC protocols at the Boston University Medical Center. Baseline plasma samples were obtained through the cephalic sinus 24 hours before bacterial inoculation. Isolates of *NTHi* grown to the mid-log phase were diluted in Hanks' balanced salt solution (HBSS), and about 25 to 75 CFU in 100 μl were introduced directly into each middle ear bullae under aseptic conditions. Daily tympanometry and otomicroscopy were performed to determine the presence of fluid in the auditory bullae and signs of infection, including bulging TM. Erythema and pictures were taken. Once abnormality was identified, the middle ear cavity was accessed 48 to 72 hours later, as described previously (49). TMs of the animals to receive the formulation were observed with the speculum of an otoscope, after which the liquid hydrogel was injected through the speculum using a soft 20-gauge, 1.8-inch catheter. A direct culture of middle ear was obtained with a calcium alginate swab and immediately streaked onto a blood agar plate. Middle ear fluid was obtained with a 22-gauge angiocatheter connected to an empty tuberculin syringe, 10 to 20 μl of middle ear fluid were diluted 1:10 in HBSS, and three serial 10-fold dilutions were prepared. One hundred microliters of each dilution was plated onto the blood agar. The lower limit of detection of viable organisms in middle ear fluid using this dilution series was 100 CFU/ml. Direct and indirect ear examination was performed every 1 to 2 days until the middle ear cultures were sterile. Serial plasma samples were obtained during the experiment to determine systemic drug levels.

Statistical analysis

Data that were normally distributed were described with means and SDs and compared using paired or unpaired Student's *t* test. Otherwise, data were presented as median ± quartiles. Comparisons between groups of proportions of outcomes were done using Fisher's exact test. Statistical analysis was conducted using OriginPro software (version 8, OriginLab). Two-tailed $P < 0.05$ was considered statistically significant.

Supplementary Material

Refer to Web version on PubMed Central for supplementary material.

Acknowledgments

We thank D. Zurakowski for the helpful discussions on statistics and experimental design.

Funding: This work was financially supported by the Center for Integration of Medicine and Innovative Technology, under U.S. Army Medical Research Acquisition Activity Cooperative Agreement subcontract #W81XWH-09-2-0001, under Massachusetts General Hospital to S.I.P.; Shereta Seelig Charitable Foundation Trust to V.S.; NIH DC015050 to D.S.K.; and Trailblazer Research Grant by the Department of Anesthesia at Boston Children's Hospital to R.Y.

REFERENCES AND NOTES

1. Hoberman A, Paradise JL, Rockette HE, Shaikh N, Wald ER, Kearney DH, Colborn DK, Kurs-Lasky M, Bhatnagar S, Haralam MA, Zoffel LM, Jenkins C, Pope MA, Balentine TL, Barbadora KA. Treatment of acute otitis media in children under 2 years of age. N Engl J Med. 2011; 364:105–115. [PubMed: 21226576]
2. Teele DW, Klein JO, Rosner B. Greater Boston Otitis Media Study Group. Epidemiology of otitis media during the first seven years of life in children in greater Boston: A prospective, cohort study. J Infect Dis. 1989; 160:83–94. [PubMed: 2732519]
3. Paradise JL, Rockette HE, Colborn DK, Bernard BS, Smith CG, Kurslasky M, Janosky JE. Ottis media in 2253 Pittsburgh-area infants: prevalence and risk factors during the first two years of Life. Pediatrics. 1997; 99:318–333. [PubMed: 9041282]
4. Acuin, J. Chronic Suppurative Otitis Media: Burden of Illness and Management Options. World Health Organization; 2004.
5. Todberg T, Koch A, Andersson M, Olsen SF, Lous J, Homøe P. Incidence of otitis media in a contemporary Danish National Birth Cohort. PLOS One. 2014; 9:e111732. [PubMed: 25545891]
6. Lanphear BP, Byrd RS, Auinger P, Hall CB. Increasing prevalence of recurrent otitis media among children in the United States. Pediatrics. 1997; 99:e1.
7. Doyle WJ, Alper CM, Seroky JT, Karnavas WJ. Exchange rates of gases across the tympanic membrane in rhesus monkeys. Acta Otolaryngol. 1998; 118:567–573. [PubMed: 9726685]
8. Prausnitz MR, Mitragotri S, Langer R. Current status and future potential of transdermal drug delivery. Nat Rev Drug Discov. 2004; 3:115–124. [PubMed: 15040576]
9. Khoo X, Simons EJ, Chiang HH, Hickey JM, Sabharwal V, Pelton SI, Rosowski JJ, Langer R, Kohane DS. Formulations for trans-tympanic antibiotic delivery. Biomaterials. 2013; 34:1281–1288. [PubMed: 23146430]
10. Hoare TR, Kohane DS. Hydrogels in drug delivery: Progress and challenges. Polymer. 2008; 49:1993–2007.
11. Qiu Y, Park K. Environment-sensitive hydrogels for drug delivery. Adv Drug Deliv Rev. 2012; 64:49–60.
12. Jia X, Colombo G, Padera R, Langer R, Kohane DS. Prolongation of sciatic nerve blockade by in situ cross-linked hyaluronic acid. Biomaterials. 2004; 25:4797–4804. [PubMed: 15120526]

13. Yeo Y, Bellas E, Highley CB, Langer R, Kohane DS. Peritoneal adhesion prevention with an in situ cross-linkable hyaluronan gel containing tissue-type plasminogen activator in a rabbit repeated-injury model. Biomaterials. 2007; 28:3704–3713. [PubMed: 17512979]
14. Higuchi T. Mechanism of sustained-action medication. Theoretical analysis of rate of release of solid drugs dispersed in solid matrices. J Pharm Sci. 1963; 52:1145–1149. [PubMed: 14088963]
15. Mortensen K, Brown W, Nordén B. Inverse melting transition and evidence of three-dimensional cubatic structure in a block-copolymer micellar system. Phys Rev Lett. 1992; 68:2340–2343. [PubMed: 10045370]
16. Hecht E, Mortensen K, Gradzielski M, Hoffmann H. Interaction of ABA block copolymers with ionic surfactants: Influence on micellization and gelation. J Phys Chem. 1995; 99:4866–4874.
17. Wang YC, Tang LY, Li Y, Wang J. Thermoresponsive block copolymers of poly(ethylene glycol) and polyphosphoester: Thermo-induced self-assembly, biocompatibility, and hydrolytic degradation. Biomacromolecules. 2009; 10:66–73. [PubMed: 19133835]
18. Yu L, Zhang H, Ding J. A subtle end-group effect on macroscopic physical gelation of triblock copolymer aqueous solutions. Angew Chem Int Ed. 2006; 45:2232–2235.
19. Zhang S, Zou J, Zhang F, Elsabahy M, Felder SE, Zhu J, Pochan DJ, Wooley KL. Rapid and versatile construction of diverse and functional nanostructures derived from a polyphosphoester-based biomimetic block copolymer system. J Am Chem Soc. 2012; 134:18467–18474. [PubMed: 23092249]
20. Iwasaki Y, Wachiralarpphaithoon C, Akiyoshi K. Novel thermoresponsive polymers having biodegradable phosphoester backbones. Macromolecules. 2007; 40:8136–8138.
21. Roy D, Brooks WLA, Sumerlin BS. New directions in thermoresponsive polymers. Chem Soc Rev. 2013; 42:7214–7243. [PubMed: 23450220]
22. Wang YC, Li Y, Yang XZ, Yuan YY, Yan LF, Wang J. Tunable thermosensitivity of biodegradable polymer micelles of poly(ε-caprolactone) and polyphosphoester block copolymers. Macromolecules. 2009; 42:3026–3032.
23. Lin-Vien, DC., Colthup, NB., Fateley, WG., Grasselli, JG. The Handbook of Infrared and Raman Characteristic Frequencies of Organic Molecules. Academic Press; 1991.
24. Pichichero ME. Acute ottis media: Part II. Treatment in an era of increasing antibiotic resistance. Am Fam Phys. 2000; 61:2410–2416.
25. Pérez-Vázquez M, Román F, Aracil B, Cantón R, Campos J. In vitro activities of garenoxacin (BMS-284756) against *Haemophilus influenzae* isolates with different fluoroquinolone susceptibilities. Antimicrob Agents Chemother. 2003; 47:3539–3541. [PubMed: 14576114]
26. Hirakata Y, Ohmori K, Mikuriya M, Saika T, Matsuzaki K, Hasegawa M, Hatta M, Yamamoto N, Kunishima H, Yano H, Kitagawa M, Arai K, Kawakami K, Kobayashi I, Jones RN, Kohno S, Yamaguchi K, Kaku M. Antimicrobial activities of piperacillin-tazobactam against *Haemophilus influenzae* isolates, including β-lactamase-negative ampicillin-resistant and β-lactamase-positive amoxicillin-clavulanate-resistant isolates, and mutations in their quinolone resistance-determining regions. Antimicrob Agents Chemother. 2009; 53:4225–4230. [PubMed: 19651910]
27. Dagan R, Leibovitz E, Greenberg D, Yagupsky P, Fliss DM, Leiberman A. Early eradication of pathogens from middle ear fluid during antibiotic treatment of acute otitis media is associated with improved clinical outcome. Pediatr Infect Dis J. 1998; 17:776–782. [PubMed: 9779760]
28. Olusanya BO. Hearing impairment in children with impacted cerumen. Ann Trop Paediatr. 2003; 23:121–128. [PubMed: 12803741]
29. Karande P, Jain A, Ergun K, Kispersky V, Mitragotri S. Design principles of chemical penetration enhancers for transdermal drug delivery. Proc Natl Acad Sci USA. 2005; 102:4688–4693. [PubMed: 15774584]
30. Simons, EJ. Chemical Penetration Enhancers and In Situ-Forming Reservoirs for Trans-Tympanic Drug Delivery: Progress Toward Improved Treatment of Otitis Media. Massachusetts Institute of Technology; 2008.
31. Bhatt PP, Hanna MS, Szeptycki P, Takeru H. Finite dose transport of drugs in liquid formulations through stratum corneum: analytical solution to a diffusion model. Int J Pharm. 1989; 50:197–203.
32. Molvær OI, Vallersnes FM, Kringlebotn M. The size of the middle ear and the mastoid air cell: System measured by an acoustic method. Acta Otolaryngol. 1978; 85:24–32. [PubMed: 626053]

33. Uhde GI. The problem of permeability and anesthesia of the tympanic membrane. AMA Arch Otolaryngol. 1957; 66:391–407. [PubMed: 13457568]
34. Wall GM, Stroman DW, Roland PS, Dohar J. Ciprofloxacin 0.3%/dexamethasone 0.1% sterile otic suspension for the topical treatment of ear infections: A review of the literature. Pediatr Infect Dis J. 2009; 28:141–144. [PubMed: 19116600]
35. U.S. Food and Drug Administration. CDER 2001 Meeting Documents. 2001. www.fda.gov/ohrms/dockets/ac/cder01.htm
36. Cheng T, Dai C, Gan RZ. Viscoelastic properties of human tympanic membrane. Ann Biomed Eng. 2007; 35:305–314. [PubMed: 17160465]
37. Van der Jeught S, Dirckx JJJ, Aerts JRM, Bradu A, Podoleanu AG, Buytaert JAN. Full-field thickness distribution of human tympanic membrane obtained with optical coherence tomography. J Assoc Res Otolaryngol. 2013; 14:483–494. [PubMed: 23673509]
38. Moghadam SH, Saliaj E, Wettig SD, Dong C, Ivanova MV, Huzil JT, Foldvari M. Effect of chemical permeation enhancers on stratum corneum barrier lipid organizational structure and interferon alpha permeability. Mol Pharm. 2013; 10:2248–2260. [PubMed: 23587061]
39. Kohane DS, Langer R. Biocompatibility and drug delivery systems. Chem Sci. 2010; 1:441–446.
40. Li Q, Wang J, Shahani S, Sun DDN, Sharma B, Elisseeff JH, Leong KW. Biodegradable and photocrosslinkable polyphosphoester hydrogel. Biomaterials. 2006; 27:1027–1034. [PubMed: 16125222]
41. Gough AW, Kasali OB, Sigler RE, Baragi V. Quinolone arthropathy—Acute toxicity to immature articular cartilage. Toxicol Pathol. 1992; 20:436–449. [PubMed: 1295072]
42. Lieberthal AS, Carroll AE, Chonmaitree T, Ganiats TG, Hoberman A, Jackson MA, Joffe MD, Miller DT, Rosenfeld RM, Sevilla XD, Schwartz RH, Thomas PA, Tunkel DE. The diagnosis and management of acute otitis media. Pediatrics. 2013; 131:e964–e999. [PubMed: 23439909]
43. Canafax DM, Giebink GS. Clinical and pharmacokinetic basis for the antimicrobial treatment of acute otitis media. Otolaryngol Clin North Am. 1991; 24:859–875. [PubMed: 1870879]
44. Barkai G, Leibovitz E, Givon-Lavi N, Dagan R. Potential contribution by nontypable *Haemophilus influenzae* in protracted and recurrent acute otitis media. Pediatr Infect Dis J. 2009; 28:466–471. [PubMed: 19504729]
45. Schmelzle J, Birtwhistle RV, Tan AKW. Acute otitis media in children with tympanostomy tubes. Can Fam Physician. 2008; 54:1123–1127. [PubMed: 18697973]
46. Pelton SI, Figueira M, Albut R, Stalker D. Efficacy of linezolid in experimental otitis media. Antimicrob Agents Chemother. 2000; 44:654–657. [PubMed: 10681334]
47. Iwasaki Y, Yamaguchi E. Synthesis of well-defined thermoresponsive polyphosphoester macroinitiators using organocatalysts. Macromolecules. 2010; 43:2664–2666.
48. Wong M, Hollinger J, Kozycz LM, McCormick TM, Lu Y, Burns DC, Seferos DS. An apparent size-exclusion quantification limit reveals a molecular weight limit in the synthesis of externally initiated polythiophenes. ACS Macro Lett. 2012; 1:1266–1269.
49. Sabharwal V, Ram S, Figueira M, Park IH, Pelton SI. Role of complement in host defense against pneumococcal otitis media. Infect Immun. 2009; 77:1121–1127. [PubMed: 19139190]

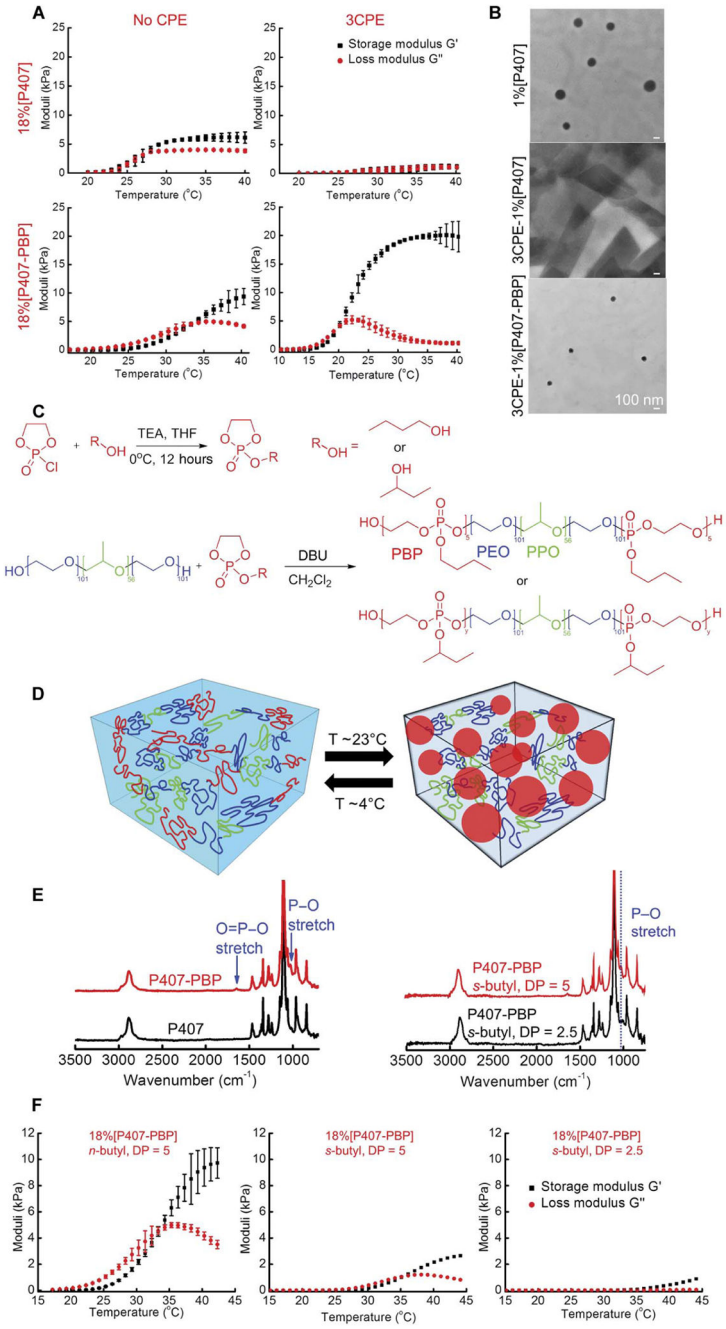

Fig. 1. Synthesis, gelation, and mechanical properties of P407-PBP

(**A**) Gelation of aqueous solutions of 18%[P407], 3CPE-18%[P407], 18%[P407-PBP], and 3CPE-18%[P407-PBP], as a function of temperature. 3CPE: 2% LIM, 1% SDS, and 0.5% BUP. Data are means ± SD ($n = 4$). (**B**) TEM images of micelle formation. Scale bars, 100 nm. (**C**) Synthesis steps for P407-PBP and chemical structures of the ABCBA penta-block copolymers. (**D**) Schematic of the gelation of P407-PBP aqueous solution, facilitated by hydrophobic interactions of PPE end groups at elevated temperature. (**E**) FTIR spectra of P407, P407-PBP with *n*-butyl groups, and P407-PBP with *s*-butyl groups. (**F**) Effect of *n*- or

s-butyl phosphoester and DP on G′ and G″ of 18% aqueous solution of P407 derivatives, as a function of temperature. Data are means ± SD ($n = 4$).

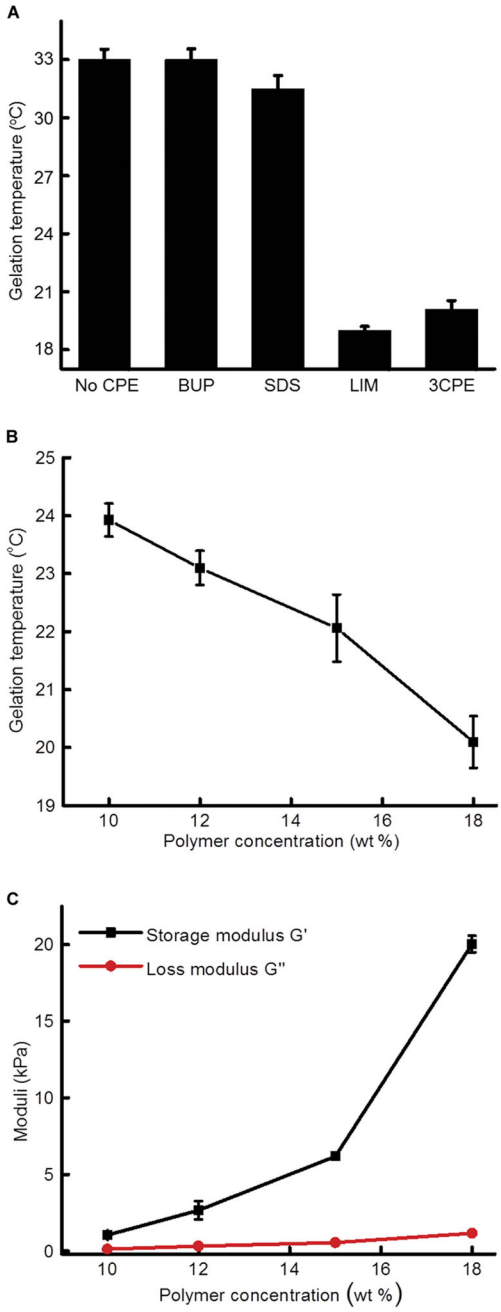

Fig. 2. Effects of individual CPEs and polymer concentrations on formulation rheology

(**A**) Effect of individual CPEs on gelation temperature of P407-PBP. (**B**) Effect of P407-PBP concentration on gelation temperature. All formulations contain 3CPE. (**C**) Effect of P407-PBP concentration on G′ and G″ at 37°C. Data are means ± SD ($n = 4$).

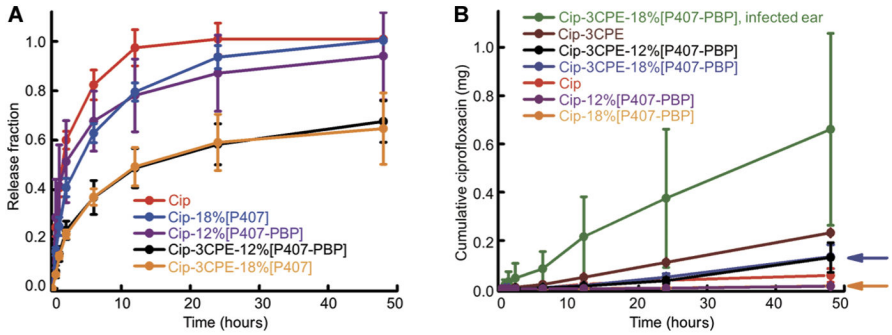

Fig. 3. Cumulative in vitro release and ex vivo transfer of ciprofloxacin across the TM into a receiving chamber

(**A**) Release of ciprofloxacin under infinite sink conditions. Two milligrams of ciprofloxacin were contained in each gel and solution at time zero. (**B**) Permeation of ciprofloxacin across the TM. The curves for Cip-12%[P407-PBP] and Cip-18%[P407-PBP] formulations overlap almost completely. The positions of the latter are indicated by arrows. Data are means ± SD ($n = 4$).

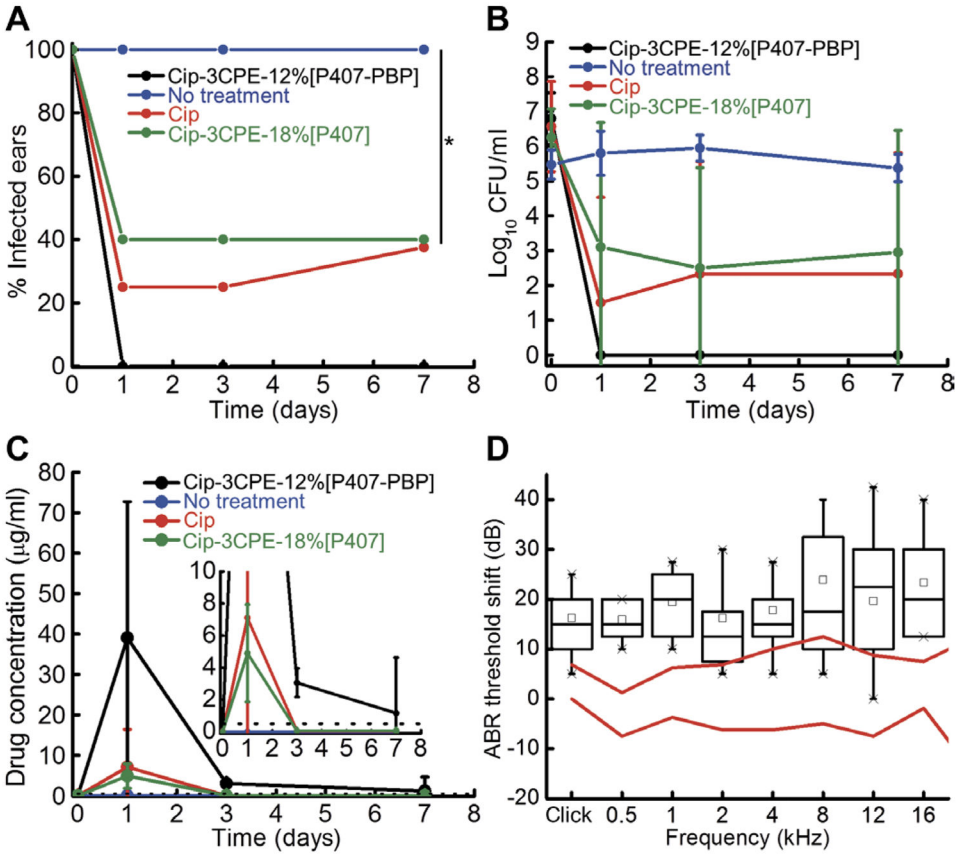

Fig. 4. In vivo efficacy, pharmacokinetics, and impact on hearing sensitivity for Cip-3CPE-12% [P407-PBP]

(**A**) Percentage of animals with OM (defined as nonzero CFU values in their middle ear fluid aspirates) before (day 0) and after receiving Cip-3CPE-12%[P407-PBP] ($n = 10$), Cip-3CPE-18%[P407] ($n = 5$), 1% ciprofloxacin ear drop ($n = 8$), or no treatment ($n = 10$). Day 0 reflects status immediately before administration of therapeutics. *$P = 0.0065$ by Fisher's exact test. (**B**) Time course of bacterial CFU from middle ear fluid from animals with OM from *NTHi* treated with Cip ($n = 4$), Cip-3CPE-18%[P407] ($n = 5$), Cip-3CPE-12%[P407-PBP] ($n = 10$), or no treatment ($n = 10$). Data are means ± SD. (Log_{10} CFU is set to zero instead of minus infinity for the purpose of this illustration.) (**C**) Concentration of ciprofloxacin over time in the middle ear fluid of the same animals as in (A). The black dotted line indicates the MIC for *NTHi*. Inset is the magnified drug concentration range of 0 to 10 μg/ml. Data are means ± SD. (**D**) Shifts in ABR thresholds in response to acoustic clicks and brief (8-ms) tone bursts of various frequencies. All data here had the threshold median before the treatment subtracted from them. The red lines indicate the interquartile range of values before treatment ($n = 8$). Measurements after application of 200 μl of Cip-3CPE-12%[P407-PBP] formulation are in black ($n = 8$). Black boxes and the lines within indicate the interquartile ranges and medians, respectively. Small black squares indicate the means, and crosses indicate the range. Original data are provided in table S4.

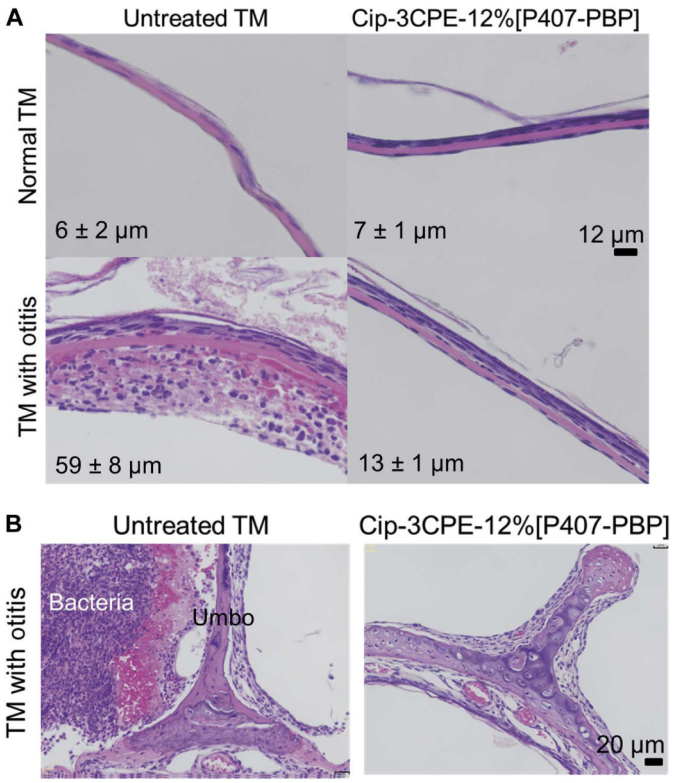

Fig. 5. In vivo effect on tissue for Cip-3CPE-12%[P407-PBP]

(**A**) Representative photomicrographs of hematoxylin and eosin (H&E)–stained sections of TM cross-sections in healthy TMs and TMs after 7 days of OM without or after treatment with Cip-3CPE-12%[P407-PBP]. Scale bar, 12 μm. Labeled on each panel is the TM's average thickness ± SD ($n = 4$). (**B**) H&E-stained cross-sections of the umbo-malleus region after 7 days of OM, without or after treatment with Cip-3CPE-12%[P407-PBP]. Scale bar, 20 μm. Thickness measurements are provided in table S4.

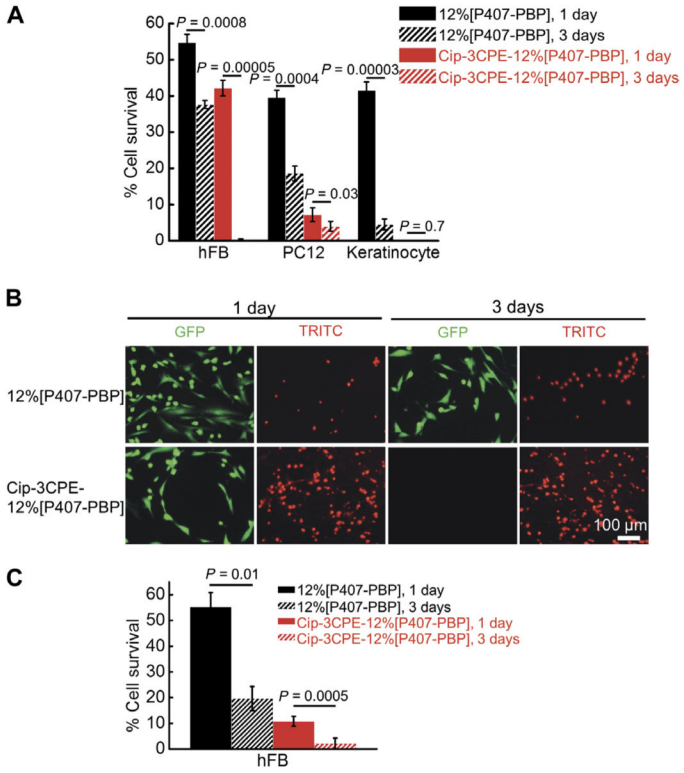

Fig. 6. Cytotoxicity of 12%[P407-PBP] and Cip-3CPE-12%[P407-PBP]

(**A**) Survival rates (determined by MTS assay) of hFBs, PC12 cells, and keratinocytes after incubating with 12%[P407-PBP] and Cip-3CPE-12%[P407-PBP] for 1 or 3 days. Data are means ± SD ($n = 4$). (**B**) LIVE/DEAD assay of hFB, which was done to confirm the data in (A), after incubation for 1 or 3 days with 12% [P407-PBP] or Cip-3CPE-12%[P407-PBP]. GFP (green fluorescent protein), live cells (green); TRITC (tetramethyl rhodamine isothiocyanate), dead cells (red). (**C**) hFB cell survival rates were obtained by counting live and dead cells in (B) and calculating % cell survival = live cells/(live cells + dead cells). Cell counting was done using ImageJ. Data are means ± SD ($n = 4$). For all images, paired *t* test was applied.